Cement and Concrete Research 40 (2010) 208–219

Contents lists available at ScienceDirect

Cement and Concrete Research

journal homepage: http://ees.elsevier.com/CEMCON/default.asp

Characterization by solid-state NMR and selective dissolution techniques of anhydrous and hydrated CEM V cement pastes

F. Brunet [a,*], T. Charpentier [a], C.N. Chao [b], H. Peycelon [b], A. Nonat [c]

[a] CEA, IRAMIS, Service Interdisciplinaire sur les Systèmes Moléculaires et Matériaux, LSDRM, F-91191 Gif sur Yvette Cedex, France
[b] CEA, DPC, Service de la Corrosion et du Comportement des Matériaux dans leur Environnement, F-91191 Gif sur Yvette Cedex, France
[c] Institut Carnot de Bourgogne, UMR 5209 CNRS-Université de Bourgogne, 9 Av. A. Savary, BP 47 870, F-21078 DIJON Cedex, France

ARTICLE INFO

Article history:
Received 5 February 2009
Accepted 2 October 2009

Keywords:
Hydration (A)
Amorphous material (B)
Blended cement (D)
NMR spectroscopy

ABSTRACT

The long term behaviour of cement based materials is strongly dependent on the paste microstructure and also on the internal chemistry. A CEM V blended cement containing pulverised fly ash (PFA) and blastfurnace slag (BFS) has been studied in order to understand hydration processes which influence the paste microstructure. Solid-state NMR spectroscopy with complementary X-ray diffraction analysis and selective dissolution techniques have been used for the characterization of the various phases (C_3S, C_2S, C_3A and C_4AF) of the clinker and additives and then for estimation of the degree of hydration of these same phases. Their quantification after simulation of experimental ^{29}Si and ^{27}Al MAS NMR spectra has allowed us to follow the hydration of recent (28 days) and old (10 years) samples that constitutes a basis of experimental data for the prediction of hydration model.

1. Introduction

Cements are widely used in the world as building materials and also for the storage and disposal of nuclear wastes in the nuclear industry. The interest of this material is due to its mechanical and chemical properties [1]. Portland cements are constituted by clinker (95%) which is a polyphasic material including calcium silicates ($Ca_3SiO_5 = C_3S$ or alite, $Ca_2SiO_4 = C_2S$ or belite), calcium aluminates and aluminoferrite at which calcium sulphate is added [2]. These cements usually contain 50–75 wt.% alite and 5–30 wt.% belite. In order to reduce CO_2 emission and also because of their interesting transport properties in the case of the use in waste disposals, blended cements and especially CEM V cements in which clinker is blended with blastfurnace slag (BFS) and pulverised fly ash (PFA) are more and more used [3,4]. Cement chemistry has been widely studied for decades and the effect of supplementary cementitious materials (SCMs) such as BFS and PFA is more recently extensively studied. However due to its complexity, the reactivity of the ternary system clinker BFS PFA is less well known. So it is crucial to understand the hydration mechanisms of these CEMV cements, and the relation between the chemical properties and the long term behaviour of this kind of material. The characterization of anhydrous constituents and the estimation of the degree of hydration of each component during time aim to constitute a basis of experimental data to predict the evolution of this cement material. Multinuclear magic-angle spinning (MAS) NMR has been successfully applied [5–10] during recent years because local structural information can be provided even in the absence of long-range structural order. ^{29}Si MAS NMR studies [11–13] have enabled to characterize the different silicate phases in the clinker and to follow the hydration reactions of alite, belite and industrial by-product additions in these cements. Due to the overlapping of resonance lines of these various compounds, their amounts are obtained by decomposition of ^{29}Si MAS NMR spectra. As CEM V cements contain relatively important quantities of aluminium (C_3A, C_4AF, PFA and BFS), it is also of interest to characterize aluminium in anhydrous CEM V cements by ^{27}Al MAS NMR [14–20] and to follow the hydration of these aluminate phases. But the difficulty for nuclei with $I>½$ like ^{27}Al is the quadrupolar interaction which leads to broadened spectra. A good improvement for resolution of different resonances may be obtained by recording ^{27}Al MAS NMR spectra at high field [9,15,20] together with high-speed spinning frequency ($\nu_r \geq 10$ kHz). ^{27}Al MAS NMR has proven to be a very useful tool to probe Al sites in cement materials since the ^{27}Al isotropic chemical shift distinguishes clearly between various tetrahedral Al (IV) or octahedral Al (VI) coordination [21,22]: indeed in the anhydrous phases (with the exception of the ferrite phase C_4AF) aluminium occurs in tetrahedral sites, whereas in the hydrated phases it occurs only in octahedral sites (except for substitution for silicon in tetrahedral sites). Furthermore the ^{27}Al quadrupole coupling parameters (C_Q and η) may give additional information about the symmetry of the electronic environment around the Al nucleus. In

* Corresponding author. Fax: +33 1 69 08 98 06.
E-mail address: francine.brunet@cea.fr (F. Brunet).

0008-8846/$ – see front matter © 2009 Elsevier Ltd. All rights reserved.
doi:10.1016/j.cemconres.2009.10.005

Table 1
Composition of the CEM V cement with the percentage in weight of different components.

	% Weight in clinker	% SiO_2	% Al_2O_3	% CaO	% Fe_2O_3	% MgO
CEM V composition	100%	27.7%	11.6%	47.1%	2.9%	2.7%
Constituent composition						
Clinker	55%	14.8%	5.3%	67.4%	2.2%	1.2%
Blastfurnace slag	22%	36.1%	10.9%	42.9%	0.7%	7.6%
Pulverised fly ash	23%	50.5%	27.4%	2.5%	6.6%	1.6%
Gypsum	5%					

Portland cements Skibsted et al. [11] have shown that ^{29}Si MAS NMR spectroscopy is a very valuable tool for quantifying the silicate phases. In this work we have characterized anhydrous CEM V and hydrated cement pastes with hydration times of 28 days, 1 year and also 10 years in order to quantify the various constituents (C_3S, C_2S, PFA and BFS) and to follow the hydration of these various phases by ^{29}Si and ^{27}Al NMR spectroscopy.

The main constituents of the CEM V used in this study are the clinker, pulverised fly ash, blastfurnace slag and gypsum as shown in Table 1 where the percentage of major components of each constituent is also reported. These data show that ^{29}Si MAS NMR should be a good method for characterizing the clinker (i.e. C_3S and C_2S) and the blastfurnace slag which are essentially constituted by SiO_2 (36%), Al_2O_3 (11%) and also CaO (42%). The ^{27}Al MAS NMR spectroscopy is complementarily well adapted for the characterization of pulverised fly ash which is very rich in Al_2O_3 (27%). ^{29}Si and ^{27}Al MAS NMR spectra of reference compounds have been recorded first for simulation of the NMR spectra of CEM V cements.

A method of selective dissolution has also been used to follow the hydration degree of the blastfurnace slag (BFS) and pulverised fly ash (PFA). Recently it was shown [23] that these two techniques are useful methods for estimating the degree of hydration of silicate and aluminate phases in cement–blastfurnace slag blends. The portlandite content in hydrated samples has also been evaluated by thermal analysis (TGA).

2. Experimental

2.1. Materials

Commercial anhydrous CEM V cement was used in this study and obtained from Holcim France Benelux. Its composition in terms of metal oxide composition is given in Table 1. Two series of hydrated samples were prepared from this cement corresponding to initial water/cement ratio of 0.3 and 0.4. For each series the hydration degrees of a recent (28 days and 1 year) and an old hydrated sample (10 years) were investigated. For the latter samples a CEMV cement from the same plant with blastfurnace slag and fly ash from the same places was used. The average composition of this cement as given by the producer was the same as the new one and the standard deviation over 1 year was less than 2%. Some additional samples were also hydrated 1, 7 and 90 days and analysed only by TGA and selective dissolution method. Samples were mixed by hand and cast in cylindrical moulds (8 cm high and 6 cm in diameter). After 24 h they were demoulded and stored at 20 °C in saturated lime solutions. The 10 year old samples were kept 1 year in a saturated lime solution and then stored in closed containers at constant temperature (20 °C and 100% of relative humidity). Before analysis, hydrated samples were ground and sieved until most of the material passed through a 63 μm sieve.

The SCMs reference samples, pulverised fly ash (PFA) and blastfurnace slag (BFS) are those used in the CEM V. The reference clinker phases (C_3A, C_4AF, alite and belite) are provided by Lafarge LCR. The samples were kept in desiccators to prevent atmospheric CO_2 contamination.

2.2. NMR measurements

^{29}Si MAS NMR spectra were collected on a Bruker DMX 300 spectrometer (magnetic field of 7.05 T) using a CPMAS probe with 7 mm o.d. ZrO_2 rotors at a spinning frequency of 5 kHz. Recycle delays of 60 s to 120 s were employed for single-pulse acquisition to ensure completely relaxed spectra and quantitative results. An estimation of the ^{29}Si spin-lattice relaxation time T_1 was derived by progressive saturation methods using recycle delays of 60 s to 600 s. The total accumulation time of a ^{29}Si spectrum was typically between 1 and 2 days. Cross-polarization ^{1}H–^{29}Si experiments were performed on hydrated samples using a recycle time of 2 s and a contact time of 1.5 ms.

^{27}Al MAS NMR spectra were acquired on a Bruker Avance 500 WB spectrometer (magnetic field of 11.75 T) using 2.5 mm o.d. ZrO_2 rotors. All experiments were acquired using a single-pulse excitation with a non selective short pulse ($\pi/12$) to ensure quantitativeness with a 2 s relaxation delay and a spinning frequency of 31.25 kHz. For C_3A and C_4AF a 4 mm o.d probe was used with a spinning frequency of 12.5 kHz.

^{29}Si and ^{27}Al chemical shifts are referenced to external samples of tetrakis (trimethylsilyl)silane (TKS) and a 1 M aqueous solution of $AlCl_3.6H_2O$, respectively. In order to perform a quantitative analysis, ^{27}Al MAS NMR spectra were fitted using a homebuilt package [24] implementing advanced features for the description of the lineshape for disordered materials [25]. Notably, in order to take into account the effects of the NMR parameter distribution, a Gaussian Isotropic Model (GIM) was used for the quadrupolar interaction and a normal (Gaussian) distribution for the isotropic chemical shift. This fitting procedure provides the mean and standard deviation value of isotropic chemical shift, and the mean value of the quadrupolar coupling parameter P_Q:

$$P_Q = C_Q\sqrt{1 + {\eta^2}/{3}}$$

where C_Q is the quadrupolar coupling constant ($C_Q = e^2qQ/h$) and η the asymmetry parameter of the electric gradient field (EFG) tensor.

2.3. XRD analysis

Anhydrous clinker was investigated by X-Ray Diffraction using a Bruker D8 diffractometer equipped with a high-speed Advance detector. A quantitative analysis of the cement has been performed from the X-ray pattern by the Rietveld method with the Topas software mainly in order to estimate the proportion of alite and belite and to compare to the Bogue calculation. The results of both calculations are given in Table 2. The contribution of each phase to the ^{29}Si and ^{27}Al NMR signal is also reported. They were calculated from the chemical analysis of each phase using the mineralogical composition.

2.4. Selective dissolution technique

The selective dissolution procedure used in this work is derived from the procedure described by Luke and Glasser [26] for

Table 2
Composition of the CEM V cement with the percentage in weight of different components and silicate phases using Bogue and Rietveld analysis.

	Proportion by weight		Repartition of Si		Repartition of Al	
Clinker	55%		29.4%		9.6%	
	Bogue	Rietveld	Bogue	Rietveld	Bogue	Rietveld
C3S	34.9%	36.4%	21.7%	23.3%	–	–
C2S	9.3%	7.1%	7.7%	6%	–	–
C3A	5.2%	5.6%	–	–	6.1%	6.1%
C4AF	5.6%	5.9%	–	–	3.6%	3.6%
Blastfurnace slag	22%		28.7%		19.3%	
Pulverised fly ash	23%		41.9%		71%	

blastfurnace slag–cement blends. Preliminary tests showed that fly ash appeared to be also insoluble in these conditions; accordingly we used this procedure to determine the amount of unhydrated material. Of course it is not possible to distinguish the fly ash from the slag in this way.

In this procedure, 125 mL of 0.1 M Na_2CO_3 solution containing also 0.05 M EDTA was prepared. 12.5 mL of a 1:1 triethanolamine: water (by volume) mixture was then added with 125 mL of water. The pH was then adjusted at 11.6 ± 0.1 with a 0.1 M NaOH solution: 0.25 g of the ground and sieved powder was added to the dissolution mixture and stirred on a vibrating table during 30 min. The residue was filtered under vacuum and dried in an oven at 105 °C during 20 h. All residual material was washed 7 times with 20 mL of distilled water then 3 times with 20 mL of methanol before being dried once again at 105 °C during 24 h and weighted. The results are corrected from the residue obtained by dissolving the clinker in the same conditions.

The ratio of slag + FA which was reacted is calculated according to

$$\%reacted\_addition = 100 - \frac{w_2 + (\%m_{addition} \times \%addition_{dissolved} \times w_1) - (\%m_{clinker} \times C_r \times w_1)}{\%m_{addition} \times w_1} \times 100$$

where:

- w_1 is the mass of sample at 1000 °C
- w_2 is the mass of the residue at 105 °C
- C_r is the percentage of residue in clinker
- $\%m_{clinker}$ is the percentage of clinker in cement by weight
- $\%m_{addition}$ is the percentage of additions in cement by weight
- $\%addition_{dissolved}$ is the percentage of dissolved additions.

2.5. Thermal analysis

TG-DTG analysis was used to quantify the amount of portlandite in the hydrated samples using a NETZSCH TG209 analyser. 10 to 15 mg of the ground and sieved powder was submitted to a linear increase of temperature from ambient to 1000 °C with a rate of 10 °C/min under a nitrogen flow (10 mL/min). The amount of portlandite was estimated from the mass loss between 420 and 510 °C which are the limits of the DTG peak in the experimental conditions, reported to the mass of the sample at 1000 °C which is assimilated to the mass of anhydrous cement.

3. Results and discussion

The composition of anhydrous CEM V cement can be determined after identification and quantification of the various amorphous and crystalline silicate phases present in this material. The amount of these various phases is obtained by decomposition of the ^{29}Si MAS NMR spectra as soon observed by Skibsted et al. for Portland cements [11–13]. The major difficulty for the analysis of the ^{29}Si MAS NMR spectra in the case of multi-component cements arose from the possible overlapping of resonance, so that the quantification procedure is rather tricky. In the present work, the method we used consists of a preliminary characterization of four reference compounds (alite, belite, BFS, PFA), yielding reference *subspectra*. Subsequently, the identification and the quantification of these various phases observed in a CEM V spectrum are obtained from its fit by the aforementioned reference subspectra. The sensitivity of the ^{29}Si being very weak, acquisition times of about 2 days were found to be necessary. In order to ensure a complete relaxation of ^{29}Si signals (for sake of quantitativeness), we have estimated by a progressive saturation method the ^{29}Si spin-lattice relaxation times T_1. They are expected to be very long T_1: from 10 s to 600 s have been previously reported [6]. The results obtained by ^{29}Si MAS NMR analysis have been compared with those obtained by Rietveld analysis of the XRD pattern and Bogue calculation.

The same method was used to investigate the ^{27}Al MAS NMR spectra for the characterization of the different anhydrous and hydrated aluminium phases present in the studied multi-component CEM V cement pastes. In addition to the isotropic chemical shift, aluminium sites in the reference compounds were also characterized by their quadrupolar interaction parameters: the quadrupolar coupling constant C_Q and quadrupolar asymmetry parameter η. Previous studies [14,15,17–21] on Portland cements have proven the high potential of ^{27}Al MAS NMR in distinguishing and characterizing the tetrahedral and octahedral coordinated aluminium, so that one can easily follow the hydration progress of the aluminate phases thanks to the chemical shift difference between the two types of Al coordination [22].

Hydration of cement proceeds in two simultaneous processes: the different phases composing the cement are dissolved, and the dissolved species precipitate to form hydrates. Silicate phases lead to the formation of calcium silicate hydrate ($CaO–SiO_2–H_2O$ i.e. C–S–H) which is the main hydration product. Aluminate phases lead to AFt and AFm phases which derive from ettringite $Ca_6Al_2(SO_4)_3(OH)_{12}\cdot 26H_2O$ and tetracalcium monosulfoaluminate hydrate $Ca_4Al_2SO_4(OH)_{12}\cdot xH_2O$) respectively. Hydration degree may therefore be estimated from the decrease in intensity of the NMR lines of anhydrous species and/or the increase of the hydrated species lines, since the resonances do not appear at the same chemical shifts. The consumption of BFS and PFA may also be estimated by a selective dissolution technique by which hydrated species and clinker phases are only dissolved. The residue corresponds to the non hydrated BFS and PFA. Finally, due to the difference in Ca/Si ratio of anhydrous silicates and C–S–H, their hydration leads to the formation of portlandite $Ca(OH)_2$. But this product may be partially consumed to also form C–S–H from BFS and PFA. It is then useful to follow the amount of portlandite in the hydrated samples by thermal analysis.

3.1. Characterization of anhydrous silicate phases by ^{29}Si MAS NMR

Chemical shifts of silicates range between −60 and −140 ppm and allow the characterization of the various tetrahedral Q^n environments, depending on their connectivity [6]. The ^{29}Si MAS NMR spectrum of belite (Fig. 1a) exhibits a single narrow (width of about 30 Hz) resonance at −71.3 ppm [8,11], in the chemical shift range for isolated SiO_4 tetrahedra (i.e.Q^0 units) and in agreement with the crystal structure of β–C_2S [27] in which all silicon atoms are equivalent. The absence of spinning sidebands is characteristic of an isotropic environment and the very long recycle delay, about 240 s, necessary for recording a fully relaxed spectrum is indicative of the absence of iron in this phase. For alite which is the major component of the clinker, the observed ^{29}Si spectrum (Fig. 1b) is broadened due to the overlapping of nine resonances of the different SiO_4 tetrahedra in the triclinic M_I form of alite [9,11] as confirmed by the XRD pattern. The lack of resolution is due to the incorporation of small quantities of impurities (Al^{3+}, Mg^{2+}, Fe^{3+} and Mn^{3+}) [13] in the crystal which distort the SiO_4 tetrahedra. Consequently, the spectrum has been simulated (Table 3) using three subspectra with peak positions at −68.9 ppm, −71.7 ppm and −73.5 ppm, and Gaussian/Lorentzian lineshapes in the intensity ratio 1/0.5/3 in agreement with the crystal structure reported for C_3S [28]. The line widths are respectively equal to about 25 Hz, 25 Hz and 40 Hz. Although the resonance lines of alite and belite are in the same chemical shift range, it is nevertheless possible to distinguish these two phases in CEM V cement and to estimate their relative proportion from the decomposition of ^{29}Si MAS NMR spectra as earlier demonstrated by Skibsted et al. [11] for Portland cements.

The spectrum (Fig. 1c) of blastfurnace slag (BFS) whose major elements are SiO_2 and CaO is characterized by a single broad line at −75.8 ppm, with intense spinning sidebands (1st and 2nd order are observed, data not shown). This corresponds to depolymerized

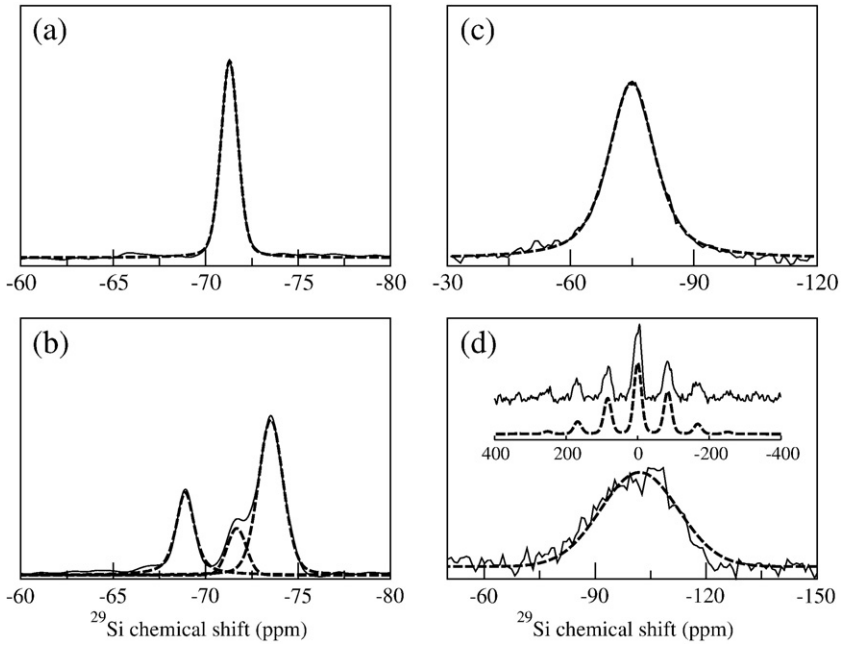

Fig. 1. Experimental (solid lines) and simulated (dashed lines) ^{29}Si MAS NMR spectra of:

a) belite C_2S
b) triclinic M_I alite C_3S
c) blastfurnace slag
d) pulverised fly ash. Inset shows the full experimental and simulated spectrum exhibiting strong spinning sidebands as a result of the iron low content. The spinning sideband pattern was simulated using a chemical shift anisotropy tensor (strength of 109 ppm and asymmetry parameter of 0.8). See text for more detail.

Each spectrum has been fitted to a Gaussian/Lorentzian lineshape with parameters given in Table 3.

aluminosilicate units. Generally, a broad resonance line is observed between −73 ppm and −75 ppm, depending on the type of slag [23,29,30], i.e. a peak at −74 ppm has been observed for anhydrous slag in the presence of chemical activators [31]. Considering the fast relaxation of the ^{29}Si signal observed in this compound, the broadening of the line (about 350 Hz) can be ascribed to the presence of a small quantity (0.7%) of paramagnetic Fe_2O_3 in this material. The chemical shift observed for blastfurnace slag (BFS) at −75.8 ppm is clearly distinct from that of C_2S at −71.3 ppm and from that of C_3S. This should allow the identification and the quantification of these different phases from the decomposition of the ^{29}Si MAS NMR spectra of cement.

The ^{29}Si spectrum of pulverised fly ash (PFA) (Fig. 1d) shows a broad resonance at −107 ppm corresponding to Q^4 tetrahedra with strong spinning sidebands (the full spectrum is shown in Fig. 1d) as a result of the presence of significant quantities of paramagnetic ion Fe^{3+} (from Fe_2O_3, 6.6 wt.%). This spinning sideband manifold (along with the significant increase of the linewidth) is a direct result of the interaction of the ^{29}Si nuclear spins with the unpaired electron spins of the Fe^{3+} ions [32] but can be also induced by an increase of the anisotropy of the bulk magnetic susceptibility as described by Kubo et al. [33]. Both effects can be well simulated with the help of chemical shift anisotropy tensor as shown in Fig. 1d. It is worth noticing that the signal to noise of the PFA was much lower than those of the other studied samples. The ^{29}Si NMR simulation parameters for the four reference compounds are reported in Table 3.

Table 3
^{29}Si NMR simulation parameters (isotropic chemical shifts δ_{iso}, Gaussian Lorentzian ratio and line widths) for the four reference compounds: belite, alite, blastfurnace slag (BFS) and pulverised fly ash (PFA) present in CEM V cement.

Compound	$-\delta_{iso}$ (ppm)	Ratio (L/G)	gb (Hz)
C3S	68.9	0.5	25
	71.7	0.5	25
	73.5	0.5	40
C2S	71.3	0.5	30
BFS	75.8	0.3	350
PFA	107	1	600

3.2. Characterization of anhydrous aluminate phases by ^{27}Al MAS NMR

It is now well established that ^{27}Al MAS NMR can be used for the characterization of complex mineralogical materials where aluminium occurs in several environments which are tetrahedral or octahedral sites [15,22,34] as in cement pastes. In anhydrous phases (tricalcium aluminate $3CaO \cdot Al_2O_3$ or C_3A) with the exception of the ferrite phase C_4AF, aluminium occurs in tetrahedral sites characterized by chemical shifts ranging from 50 to 100 ppm [13,14,19,22]. Adversely in hydrated phases aluminium occurs in octahedral sites characterized by a chemical shift range from +20 to −10 ppm [14,19]. AlO_5 units have been also observed between 30 ppm and 40 ppm [16,19–21]. The experimental ^{27}Al MAS NMR spectrum of the tricalcium aluminate C_3A is shown Fig. 2a. It displays two overlapping central transitions from the two tetrahedral coordinated Al sites in agreement with the crystal structure of C_3A. The fit of the spectrum yields the NMR parameters for the two Al (I) and Al (II) sites: $\delta_{iso} = 81.4$ ppm, $C_Q = 8.9$ MHz, $\eta = 0.32$ and $\delta_{iso} = 81$ ppm, $C_Q = 9.5$ MHz and $\eta = 0.56$, respectively (Table 4a). These values are very close to those previously reported by Skibsted et al. [14,34] and Massiot et al. [35], except for the isotropic chemical shift δ_{iso} which is found here to be slightly higher. This could be ascribed to the incorporation of impurity ions in very weak quantities, such as for instance Al^{3+} which may be substituted by Fe^{3+}.

Oldfield et al. [36] have shown that the presence of ferromagnetic Fe_3O_4 or antiferromagnetic Fe_2O_3 leads to a significant increase of the intensities and number of spinning sidebands [36,37]. Skibsted

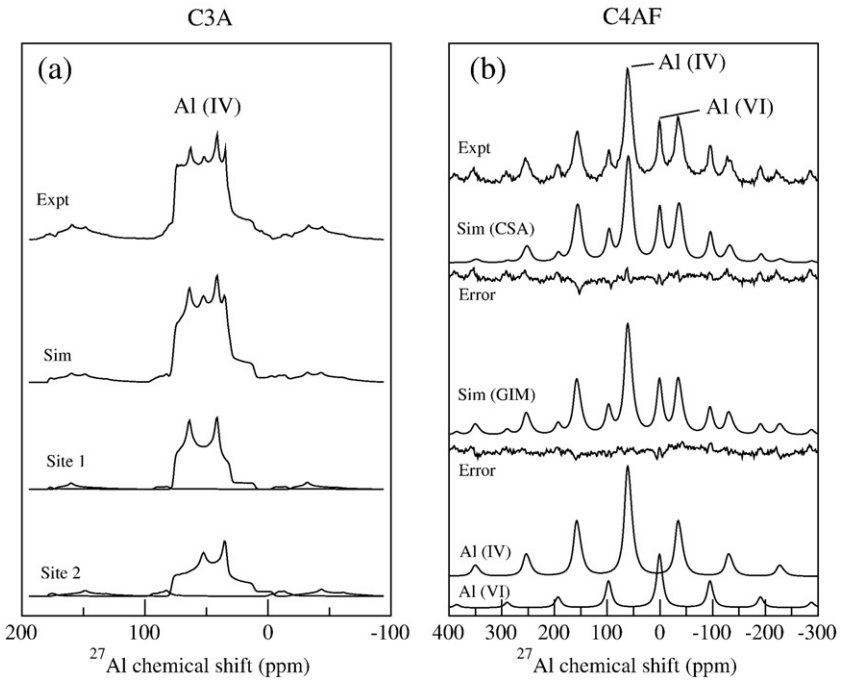

Fig. 2. Experimental and simulated ^{27}Al MAS NMR spectra of:

a) C_3A tricalcium aluminate

b) C_4AF calcium aluminoferrite. Comparison between experimental and simulated ^{27}Al MAS NMR spectra using two models (CSA and GIM, see text for description). The contribution for each site (Al (IV) and Al (VI)) is displayed at the bottom. At the top of the figure, the isotropic line for each site is indicated, other lines are spinning sidebands.

The parameters used for simulation are given in Tables 4a and 4b.

et al. [38] have also shown that the ^{27}Al nucleus–Fe^{3+} unpaired electron dipolar coupling gives a severe line broadening in ^{27}Al MAS NMR spectra, with possibly an intensity loss. Consequently, aluminium in the ferrite phase C_4AF is expected to be more difficult to detect because of its high Fe^{3+}content. However, in this sample, we observe (Fig. 2b) two relatively well-separated aluminium broad resonances at about 70 ppm and 9 ppm, but with an intense spinning sideband manifold. A similar ^{27}Al MAS spectrum was earlier described by Skibsted et al. [38] on synthetic calcium aluminoferrites. The resonances at 70 ppm and 9 ppm are attributed to Al (IV) in tetrahedral sites and to Al (VI) in octahedral sites, respectively. The crystalline structure of Ca_2AlFeO_5 contains octahedral (Fe, Al) O_6 and overall tetrahedral (Fe, Al) O_4 [39] with estimated site occupancies which are about $Fe_{0.76}Al_{0.24}O_6$ and $Fe_{0.24}Al_{0.76}O_4$. Generally the intensity loss for the ^{27}Al signal increases with augmentation of the Fe_2O_3 content. In this sample, the two sites can be well observed, as a result of the relatively low concentration of Fe_2O_3 (about 6.5%). Two models have been compared to fit the C_4AF spectrum. In a first approach (denoted CSA in Fig. 2b), we have used Gaussian lines including for both sites Al (IV) and Al (VI) including Lorentzian broadening and a chemical shift anisotropy for reproducing the observed strong spinning sidebands pattern. The chemical shift anisotropy (CSA) together with the Lorentzian broadening is in fact reflective of the ^{27}Al–Fe^{3+} electron dipolar coupling (as already mentioned for ^{29}Si, paramagnetic couplings affect the overall MAS NMR spectrum lineshape such having the spectral appearance of a CSA pattern). It was found that both lines could be well fitted using the same CSA interactions and Lorentzian broadening. This yielded parameters given in Table 4b. The fact that the Gaussian width contribution Al (VI) line is much narrower than the one of Al (IV) and because the Al (VI) was found to be slightly asymmetric, we have made an attempt to include a quadrupolar

Table 4a
^{27}Al NMR simulation parameters (δ_{iso}, asymmetry parameter η and quadrupolar coupling constant C_Q) for the three reference compounds: C_3A, BFS and PFA present in CEM V cement.

Compound		δ_{iso} (ppm)	η	C_Q (MHz)	%	References
C3A	Al (I)	81.4	0.32	8.9	50%	[a]
	Al (II)	81	0.56	9.5	50%	
	Al (I)	80	0.33	8.7	50%	[33]
	Al (II)	77.8	0.54	9.3	50%	
	Al (I)	79.5	0.32	8.7		[5,14]
	Al (II)	78.3	0.54	9.3		
BFS	Al (IV)	74.3	0.62	6.9	100%	[a]
PFA	Al (IV)	63	0.61	6.1	65%	[a]
	Al (VI)	8	0.61	5.7	35%	

[a] Our values.

Table 4b
^{27}Al NMR simulation parameters used to fit the C_4AF spectrum.

Compound	δ_{iso} (ppm)	gb (ppm)	lb (ppm)	CSA (ppm)	η csa	%
C4AF						
Model CSA (a)						
Al (IV)	59.9	4	12.5	−208	1	71%
Al (VI)	0.5	0.2	12.5	−208	1	29%
	δ_{iso} (ppm)	gb (ppm)	lb (ppm)	P Q (ppm)		%
Model GIM + spinning sidebands (b)						
Al (IV)	66	0.2	12.5	3.7		71%
Al (VI)	3.5	0.2	12.5	2.2		29%

– Model CSA (a): as a constraint, the same CSA and lb parameter was used for both sites for describing the Al–Fe coupling effects.
– Model GIM + spinning sideband manifold (b): as a constraint, lb parameter was used for both sites for describing the Al–Fe coupling effects.

parameter distribution. This could be expected from the random Fe/Al substitution which would lead to a disordered electric field gradient (EFG) over the sample. For the latter, we have used a Gaussian Isotropic Model [25]. As shown in Fig. 2b, this yielded a slightly better fit of the experimental spectrum (the discrepancy as measured by χ^2 was found to decrease by a factor of 2) but satisfactorily, the same population ratio Al (IV)/Al (VI) was obtained. The ^{27}Al NMR parameters used to fit the C_4AF spectrum are given in Table 4b. The occupancy of the octahedral coordinated aluminium Al (VI) site is of about 29%. This is in very good agreement with the estimated (about 24%) site occupancies in the crystal structure for Ca_2AlFeO_5 [39]. With the present data, it is difficult to further discuss the quadrupolar contribution to the width of each line but the use of 2D NMR MQMAS experiments could be appropriate to address this question, or MAS NMR measurements at different magnetic fields [32]. In this synthetic sample of ferrite the content of Fe_2O_3 is low (6.5%) and hence the loss of ^{27}Al NMR signal intensity is relatively weak. Generally in most ferrites, as a result of the high content of Fe_2O_3 (20% to 35% in weight), only a small proportion of the expected intensity is observed on the ^{27}Al MAS NMR spectrum and hence a quantitative estimation for the Al (IV)/Al (VI) ratio is rather difficult.

For blastfurnace slag (BFS), Fig. 3a (bottom), we observe a single asymmetric broad resonance line at about 74 ppm corresponding to Al (IV). The spectrum is of relatively good quality probably due to the fact that this industrial by-product contains a very weak quantity of iron (0.7%), and the significant increase of the spinning frequency employed (31.25 kHz). The range of chemical shifts for tetrahedral aluminosilicates is generally around 70–85 ppm which would correspond to the structure of blastfurnace slag (BFS). The aluminium inside the anhydrous slag is on a tetrahedral site and has been soon observed at this same chemical shift at high field [31]. This asymmetric and broad line is typical of disordered sites, so that we used our procedure (see Experimental Section) for fitting the spectrum. This yielded mean values of the quadrupolar coupling parameter and isotropic chemical shift of $C_Q = 6.9$ MHz and $\delta_{iso} = 74.3$ ppm, respectively (Table 4a). The same kind of lineshapes was observed in pulverised fly ash (PFA) Fig. 3a (top), for two resonances around 60 ppm and 5 ppm. For this sample, it was observed that the ^{27}Al relaxation was fast and the spinning sideband manifold was more intense, which is indicative of an important quantity of iron (about 6.6%) present in this material. These resonances are respectively attributed to Al (IV) in tetrahedral site and to Al (VI) in octahedral site. The NMR parameters as provided by the fit of the spectrum are presented in Table 4a: Al (IV): $\delta_{iso} = 63$ ppm and $C_Q = 6.1$ MHz; Al (VI): $\delta_{iso} = 8$ ppm and $C_Q = 5.7$ MHz. An approximate estimation of the intensities of the resonance lines in the ^{27}Al MAS NMR spectrum of pulverised fly ash indicates a predominance of Al^{3+} ions in the tetrahedral sites (about 65%).

3.3. Composition of the anhydrous CEMV

To determine the composition of the anhydrous CEM V samples from ^{29}Si and ^{27}Al MAS NMR, their spectra were decomposed using the subspectra of the reference compounds (Figs. 1, 2 and 3a) but taking into account an additional line broadening arising from the presence of impurities or paramagnetic ions due to the clinkerization process. The aim of this method is to quantify the silicate and aluminate phases in this type of cement, previously described by Skibsted et al. [11] for Portland cements.

3.3.1. ^{29}Si MAS NMR

On the experimental ^{29}Si MAS NMR spectrum of the anhydrous CEM V cement (Fig. 4) appears a broad resonance line around −73.3 ppm due to alite and a narrow line at −71.3 ppm due to belite. A shoulder at −75.8 ppm arising from blastfurnace slag (BFS) is also seen. The very broad resonance around −100 ppm arises from Q^4 sites of pulverised fly ash (PFA). The spinning sidebands (not shown here) are due to the presence of BFS and PFA and the relaxation of ^{29}Si

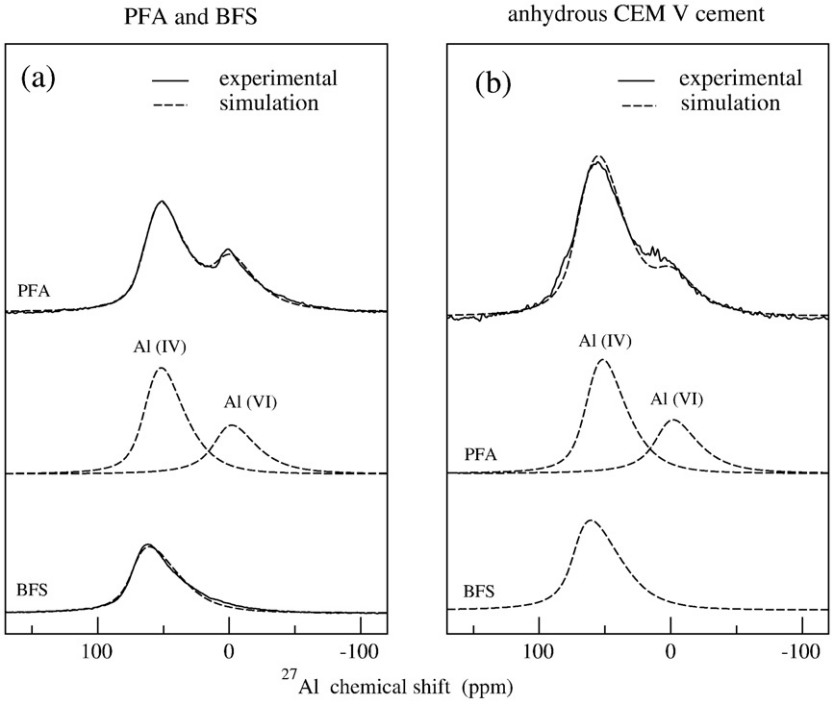

Fig. 3. Experimental and simulated ^{27}Al MAS NMR spectra acquired at MAS frequency of 31.2 kHz:

a) pulverised fly ash and blastfurnace slag. Each spectrum has been simulated using quadrupolar parameters given in Table 4a

b) anhydrous CEM V. The spectrum has been simulated from quadrupolar parameters of PFA and BFS (Table 4a).

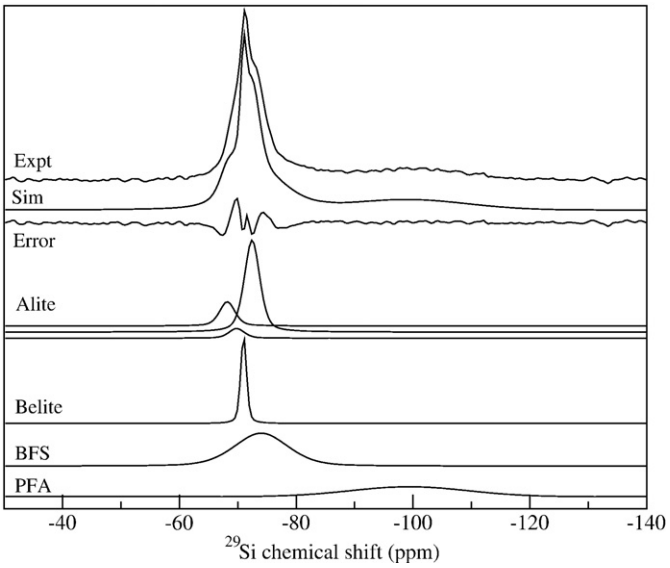

Fig. 4. ^{29}Si MAS NMR experimental and simulated spectra of anhydrous CEM V cement. Error corresponds to the difference between the two spectra. The simulated subspectra of alite, belite, blastfurnace slag and pulverised fly ash are presented below. Their simulation parameters are given in Table 3. The composition of anhydrous cement is given is given in Table 5.

resonances is faster in these two materials due to the presence of iron. The spectrum of the CEM V cement is hence composed by the subspectra of alite (C_3S), belite (C_2S), blastfurnace slag (BFS) and pulverised fly ash (PFA). The simulated spectrum (Fig. 4) of the CEM V cement is obtained from the four simulated subspectra as previously described but taking into account the fact that the line widths and positions in the ^{29}Si MAS NMR spectrum of CEM V cement may differ from references due to the clinkerization process. These effects have been taken into account by allowing line broadening of ^{29}Si resonances from alite and belite with the Fe_2O_3 content of cement and allowing slight variations of the chemical shift for pulverised fly ash resonance. Such a procedure has been already used by Skibsted et al. [11] for the quantification of silicate phases in Portland cements from completely relaxed ^{29}Si signals. The repartition of the silica among the four silica materials is obtained by decomposition of the ^{29}Si MAS NMR spectra taking into account the intensities of spinning sidebands in the main resonances for blastfurnace slag (BFS) (about 40% of the main resonance) and pulverised fly ash (PFA) (about 70%). The intensities of spinning sidebands can be neglected for the two other phases, alite and belite. The proportions are about 24% in alite, 6% in belite, 31% in blasfurnace slag (BFS) and 38% in pulverised fly ash (PFA) (Table 5). Nevertheless these values must be taken with carefulness for the method is derived from simulation of resonance lines which are slightly overlapping. The molar belite/alite ratio is about 0.25, in good agreement with the value obtained by XRD of 0.19 by weight, i.e. 0.26 molar ratio, for slightly different compositions of alite and belite. These values derived from NMR and XRD analysis fairly well agree with the calculated percentage of SiO_2 from the composition of the CEM V cement (Table 2). The agreement between XRD analysis and NMR results confirms the validity of parameters used for the decomposition of NMR spectra and demonstrates that ^{29}Si MAS NMR can be a valuable tool for quantifying alite, belite and other silicate phases in multicomponent cements. This useful method requires completely relaxed ^{29}Si signals combined with the simulation from ^{29}Si MAS NMR subspectra of reference compounds.

Against the Bogue analysis the amounts of alite and of belite are respectively equal to about 22% and 7% which gives a ratio for belite/alite equal to 0.31. This ratio is relatively higher than for other previous determinations but this calculation generally overestimates the belite content at the expense of alite as it was soon shown in Portland cements [11]. The greater discrepancies with the calculated repartition (Table 2) concern the BFS (31% comparatively to 29%) and PFA (38% comparatively to 42%). BFS and PFA have the broadest lines and an underestimation of PFA is probable.

3.3.2. ^{27}Al MAS NMR

The ^{27}Al spectrum for the anhydrous CEM V cement (Fig. 3b) shows an intense resonance around 60 ppm attributed to Al (IV) in Td site, mainly in pulverised fly ash and in slag, and another broad resonance around 5 ppm corresponding to Al (VI) in Oh site in the pulverised fly ash and in C_4AF phase in agreement with our previous observations and other data [38]. From the estimation of the relative proportion of the different aluminated compounds present in the cement (Table 2), it appears that the amount of aluminium present in the pure calcium aluminium phases as C_3A and C_4AF is weak (6% and less than 4% respectively) and that it is essentially present in pulverised fly ash (PFA) (71%) that are particularly rich in aluminium and also in blastfurnace slag (BFS) (19%). Indeed the spectrum of anhydrous CEM V cement (Fig. 3b) looks like spectra of PFA and BFS shown in Fig. 3a. Previous ^{27}Al MAS NMR studies [15] on Portland cements have shown that Al^{3+} ions can substitute Si^{4+} in the calcium silicates as alite and belite, to about 1 wt.% Al_2O_3 in clinker, so that it can be fully neglected in CEMV. Taking into account these data, the experimental spectrum of anhydrous CEM V was simulated from the two spectra of PFA and BFS (Fig. 3b) and with the following intensity constraint for the ratio Al(IV)/Al(VI) about equal to 65%/35% for PFA. The advantage of experiments at high MAS frequency (31.25 kHz) is that there are no spinning sidebands. Fig. 3b shows the relatively good agreement between experimental and simulated spectra (except the presence of few fine lines probably due to hydrated products). Results presented in Table 6 are given within ±5% and are therefore only semi-quantitative. These values are slightly different from those given for the composition of the CEM V cement (Table 2). Nevertheless they show that aluminium is essentially incorporated in pulverised fly ash (PFA). Our results from ^{27}Al MAS NMR simulated spectra confirm previous observations [13,40,41] on anhydrous aluminate phases

Table 5
Percentage of different silicate phases (C_3S, C_2S, BFS and PFA) present in anhydrous and hydrated CEM V cement from simulation of ^{29}Si NMR MAS spectra.

Species	C3S	C2S	BFS	PFA	Q^1	Q^2 (1Al)	Q^{2p}	Q^2	Hydrates
Initial	24%	6%	31%	38%					
$w/c=0.3$									
28 days	4%	5%	21%	36%	10%	7%	6%	12%	35%
1 year	4%	4%	20%	28%	10%	10%	8%	16%	44%
10 years	3%	3%	18%	27%	12%	11%	9%	18%	50%
$w/c=0.4$									
28 days	2%	5%	17%	30%	10%	9%	9%	18%	46%
1 year	1%	4%	16%	28%	10%	12%	10%	20%	52%
10 years	1%	2%	13%	27%	4%	15%	13%	26%	58%

Table 6
Percentage of different aluminate phases (BFS, PFA, ettringite and C–S–H–Al) present in anhydrous and hydrated CEM V cement from simulation of ^{27}Al NMR MAS spectra.

Species	Anhydrous	$w/c=0.4$	$w/c=0.4$
		28 days	10 years
Al (IV) BFS	31%	3%	3%
Al (IV) PFA	45%	40%	36%
Al (VI) PFA	24%	22%	20%
Al (VI) ettringite		26%	25%
Al (IV) C–S–H–Al		9%	15%
% Al (IV)	76%	52%	54%
% Al (VI)	24%	48%	45%

showing that aluminium are essentially present in tetrahedral sites (80%) contrary to octahedral sites (20%).

3.4. Composition of the hydrated CEM V pastes

3.4.1. ^{27}Al MAS NMR

Previous ^{27}Al MAS NMR studies [17–21] have shown that the hydration of calcium aluminate phases can be followed from the resolution of tetrahedral and octahedral coordinated Al species [22]. In particular the Al (VI)/Al (IV) ratio provides a good estimate of the progress of the hydration reaction of the aluminate phases. In this work we made an attempt to follow more accurately the hydration of aluminate phases from the behaviour of individual reference compounds. The spectra of hydrated ($w/c = 0.4$) CEM V samples at 28 days and 10 years shown on Fig. 5a are quite different from those observed for the anhydrous CEM V sample (Fig. 3b): a narrow resonance near 13 ppm is clearly visible and attributed to hydration products such as AFt phases according to literature data [14], AFm and hydrated magnesium aluminate such as hydrotalcite which were identified on XRD patterns. The very broad resonance near 65–75 ppm arises from blast-furnace slag (BFS) and fly ash (PFA). The experimental spectrum observed at 10 years was hence simulated using the NMR parameters of these two reference compounds, as previously determined (Tables 4a and 4b) and considering a narrow contribution (13 ppm) arising from hydrated aluminate phases. It was also necessary to consider another resonance at about 74 ppm, which was found to significantly improve the fit. We assign this broad resonance ($\delta_{iso} = 74$ ppm $C_Q = 3.7$ MHz and $\eta = 0.60$) to tetrahedral aluminium Al (IV) sites incorporated in the C–S–H [8,9,15,29,49]. This assignment is supported by the observation of the Q^2 (1Al) resonance in ^{29}Si MAS NMR spectra of Portland cements where aluminium preferentially substitutes for tetrahedral coordinated Si in the C–S–H chains [9]. The simulated spectrum shown on Fig. 5a is in relatively good agreement with the experimental spectrum at 10 years and the individual simulated spectra are presented on Fig. 5b. For the resonance at 13 ppm, the quadrupolar parameters extracted from our simulation ($\delta_{iso} = 13$ ppm, $C_Q = 1.8$ MHz and $\eta = 0.60$) are quite in agreement with the data from literature [14] for ettringite. ^{27}Al MAS NMR results demonstrate that the substitution cannot be neglected and that a more accurate description of the evolution of anhydrous and hydrate aluminates can be obtained from simulation of ^{27}Al spectra. A semi-quantitative estimation of percentage Al in the hydrated phases (Table 6) indicates that after 10 years, 15% of Al is incorporated in C–S–H when 25% is in ettringite and AFm. From these values, the Al/Si ratio in C–S–H may be evaluated to 0.11. In addition, the proportion of tetrahedral coordinated Al (IV) has greatly decreased from about 80% in the anhydrous CEM V cement to approximately 45% in the hydrated cement after 1 month without notable modification after 10 years. The most striking feature is the consumption of BFS of which the percentage has clearly decreased, contrary to PFA that are much less consumed. This worthwhile NMR result (Table 6) indicates a rather different behaviour for the two SCMs. The quantity of Al incorporated in the C–S–H has been determined directly by simulation of ^{27}Al MAS NMR spectra whereas a more complex and indirect simulation would be used for simulation of ^{29}Si MAS NMR spectra.

3.4.2. ^{29}Si MAS NMR

The ^{29}Si MAS NMR experimental spectrum of the hydrated CEM V ($w/c = 0.3$, 10 years) displayed on Fig. 6a is quite different from the ^{29}Si MAS NMR spectrum of the anhydrous cement sample (Fig. 4). We observe a narrow resonance at −71.3 ppm due to belite, a resonance at −73.3 ppm from alite and a broad shape of unresolved resonances with peaks at about −81.4 ppm and −84.3 ppm which are attributed to Q^n unit tetrahedra [13,42,43] of the calcium silicate hydrate (C–S–H) formed by hydration of the cement. This study only aims at differentiating the anhydrous and hydrated phases of the CEM V sample,

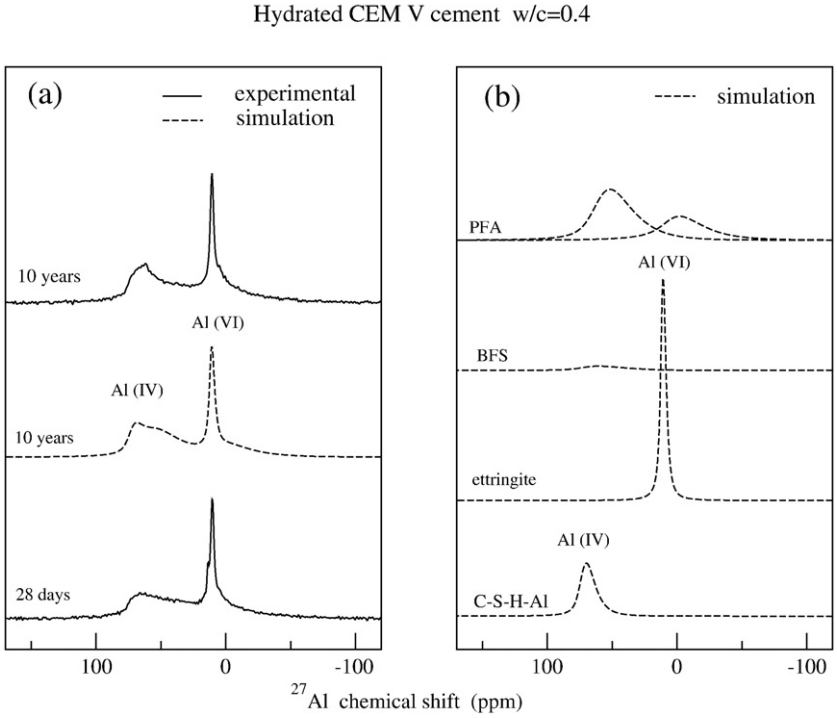

Fig. 5. ^{27}Al MAS NMR experimental (solid lines) and simulated (dashed lines) spectra of samples of:

a) hydrated cement at $w/c = 0.4$ after 28 days (bottom) and 10 years (top). MAS frequency was 31.2 kHz.

b) Simulated spectrum after 10 years (middle) whose individual components are presented at right (b) and correspond to PFA, BFS, ettringite and C–S–H–Al. The composition is given in Table 6.

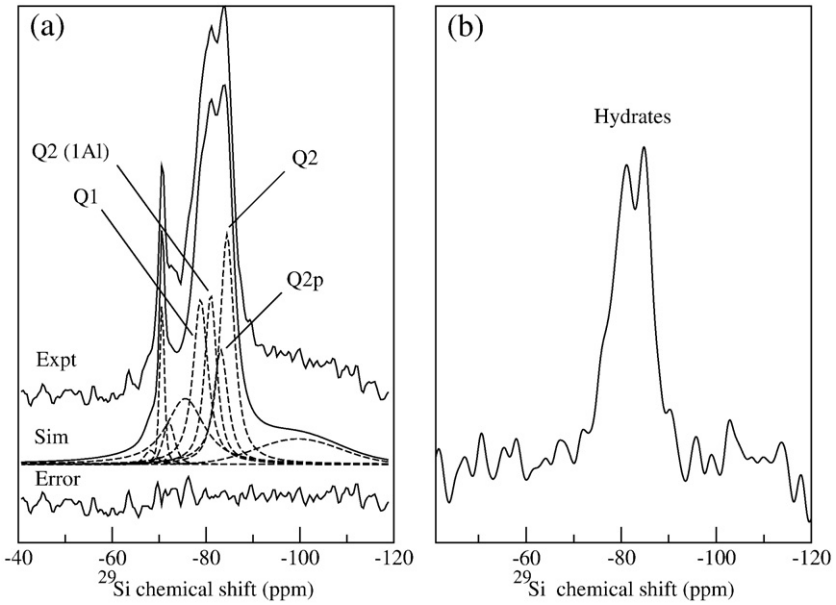

Fig. 6. ^{29}Si MAS NMR spectra of samples of hydrated cement at $w/c = 0.3$ and 10 years.

a) Experimental (solid lines) and simulated (dashed lines) spectra.
b) Experimental spectrum recorded using a cross-polarization sequence.

The compositions are given in Table 5.

so that a detailed identification of the different Q^n units will not be presented here. For such an investigation, ^{1}H–^{29}Si cross-polarization (CP) experiment is a very useful tool because it allows one to selectively observe the silicon sites close to proton sites, such as in H_2O molecules or in OH groups. The comparison of the spectrum Fig. 6a (direct acquisition) with Fig. 6b (cross-polarization) confirms the attribution of broadened lines to C–S–H sites; the resonance lines at −71.3 ppm and −73.3 ppm belonging to alite and belite are no more visible in Fig. 6b. As the hydration time increases, the intensities of the resonances at −71.3 ppm and −73.3 ppm decrease and result in an increase of the intensities for the resonances from the C–S–H phase at $w/c = 0.4$ (Fig. 7a and b). The structure of calcium silicate hydrates (C–S–H) has been the subject of numerous ^{29}Si MAS NMR studies [13,42–46] showing that the chains of silicate tetrahedral consist of a three-unit repetition pattern with an end-chain tetrahedral Q^1 resonating at −79.5 ppm, bridging tetrahedral Q^{2p} at −82.6 ppm and

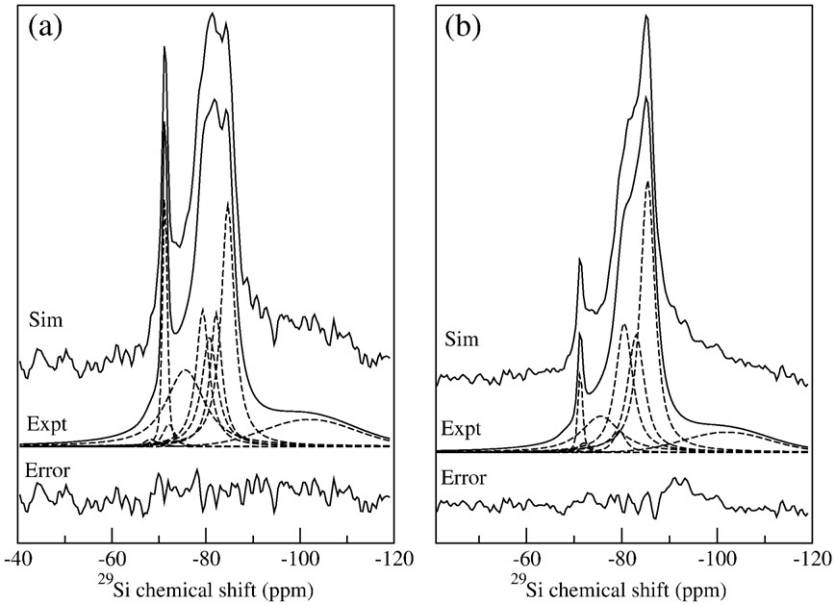

Fig. 7. ^{29}Si MAS NMR experimental (solid lines) and simulated spectra (dashed lines) of samples of:

a) hydrated cement at $w/c = 0.4$ and 28 days
b) hydrated cement at $w/c = 0.4$ and 10 years.

The compositions are given in Table 5.

nonbridging Q^2 at −85 ppm. Recent Double Quantum ^{29}Si–^{29}Si experiments [46] have revealed the connectivities between the different tetrahedral units along the chains. It is well known that the substitution of silicon by aluminium in the silicate network causes a low field shift from about 3–5 ppm of neighbouring silicon sites [6,47] and is confirmed by ^{27}Al MAS [16,19–21,48]. However, the positions of the Q^{2p} and Q^2 (1Al) resonances are often too close so that their assignment is often not obvious. The resonance line for Q^2 (1Al) has been proposed to be about −81.4 ppm [18–21]. The ^{29}Si NMR spectra have been decomposed from the spectral parameters of alite, belite, blast-furnace slag, pulverised fly ash and also from the four resonance lines Q^1, Q^{2p}, Q^2(1Al) and Q^2 of the C–S–H. Only slight variations in the chemical shifts and line widths have been taken into account in the simulations because of the probable incorporation of impurities or paramagnetic ions (mainly Fe^{3+}) in the cement. For a greater confidence in these complex simulations two constraints were taken into account. It was first assumed that the "dreierketten model" for C–S–H could be retained, so that the ratio between Q^{2p} and Q^2 intensities is equal to ½. Secondly using the following equation:

$$Al/Si = {}^1/_2\, Q^2(1Al) \,/\, \left[Q^1 + Q^{2p} + Q^2 + Q^2(1Al)\right]$$

given by Richardson et al. [48] and Andersen et al. [19] for the degree of Al substitution in the tetrahedral chains (Al IV/Si), a supplementary relation between the intensities of the Q^1, Q^{2p} and Q^2 (1Al) could be obtained from the Al/Si ratio. That is for $w/c = 0.4$ the calculated values of Al/Si at 28 days (0.095) and 10 years (0.124). This allowed a better adjustment on the positions and linewidths of the various sites Q^i. The experimental and simulated spectra are presented in Fig. 7a and b. The obtained isotropic chemical shifts (δ_{iso} (ppm) and Gaussian broadening gb (ppm)) found were then used for the simulation of other ^{29}Si spectra ($w/c = 0.3$ at 28 days, 1 and 10 years). This yielded values of Al/Si from about 0.10 to 0.11 supporting our hypothesis. From ^{29}Si NMR simulations of the six hydrated samples ($w/c = 0.3$ and 0.4) the mean values obtained for the chemical shifts are respectively -82.6 ± 0.2 ppm for Q^{2p} and -80.8 ± 0.4 ppm for Q^2 (1Al). Those values are in agreement with previous studies reported in literature [18–21,46]. The hydration evolution is clearly visible on Fig. 7a and b showing an increase of the quantity of formed hydrates (C–S–H). This quantitative estimation of the various silicate components is presented in Table 5. The present analysis of the ^{29}Si MAS NMR spectra indicates that the Al/Si ratio varies from about 0.10 to 0.12 for all hydrated samples. But as the intensities of individual resonance lines are given with uncertainties of about ±5%, it follows that the Al/Si ratio given by ^{29}Si NMR must be considered with care. Nevertheless these values which are in agreement with those obtained by ^{27}Al MAS NMR can be considered as relatively typical values for such systems.

3.4.3. Evolution of the percentage of the different phases with hydration time

The simulation of the ^{29}Si and ^{27}Al NMR spectra allows quantifying the percentage of reaction of each component of CEMV during the hydration of the pastes. Moreover, it is also possible to evaluate for SCMs the reaction of the aluminate and silicate parts separately. The percentage of reaction of each component or part of component is expressed as $100 - \alpha_{component}$ (%) where:

$$\alpha_{component}(t) = Int.(t)_{component} \,/\, Int.(t_0)_{component}$$

with:

Int. (t) = Si or Al relative intensity for the component at time t (28 days, …) in the CEM V hydrated paste.

Int. (t_0) = Intensity for the component in the anhydrous CEM V cement.

Table 7
Hydration degree: $1 - \alpha$ (%) for silicate and aluminate phases at different hydration times (28 days, 1 and 10 years) and for $w/c = 0.3$ and 0.4.

Species	C3S	C2S	BFS	PFA	BFS*	PFA*
$w/c = 0.3$						
28 days	83%	17%	33%	5%		
1 year	83%	33%	35%	26%		
10 years	88%	50%	42%	29%		
$w/c = 0.4$						
28 days	93%	17%	45%	21%	90%	10%
1 year	96%	50%	48%	26%		
10 years	96%	67%	58%	29%	90%	19%

*Aluminate part.

The percentage of reaction of each component or part of component is reported on Table 7.

After 1 month, most of alite is consumed, the percentage of reaction reaches 93% at $w/c = 0.4$ but at this stage only 17% of belite is hydrated and the degree of hydration increases after 10 years to 50 and 67% at $w/c = 0.3$ and 0.4 respectively. Concerning BFS, the silicate part follows the same trend as belite does, after 28 days 33% is consumed at $w/c = 0.3$ and 45% at $w/c = 0.4$. On the contrary, the aluminate part of BFS is nearly fully hydrated (90%) at 28 days and does not change with time anymore. This can be explained by a heterogeneity of the slag with probably more reactive aluminium richer regions. Concerning the PFA, hydration of both its silica and alumina parts is very limited; it begins from about 5% at 28 days ($w/c = 0.3$) to reach a maximum of about 30% for the silica part and no more than 20% for the aluminate part ($w/c = 0.4$).

^{27}Al MAS NMR spectra (Figs. 3b and 5a) show an important evolution of the hydration reaction in the aluminate phases without notable modification between 1 month and 10 years. Taking into account the uncertainties due to fit parameters, it follows that the values deduced from ^{29}Si and ^{27}Al NMR measurements are in relatively good agreement for they indicate that after 1 month hydration time the mean proportion of hydrated phases represents about 50% and that this ratio remains about constant after a long time of hydration (10 years).

The variation of the hydration degree of the CEM V hydrated paste constituents derived from the fits of the ^{29}Si and ^{27}Al NMR spectra is compared to the evolution deduced from the dissolution method and to the evolution of the portlandite content on Fig. 8 for water/cement ratio equal to 0.3 and Fig. 9 for water to cement ratio equal to 0.4.

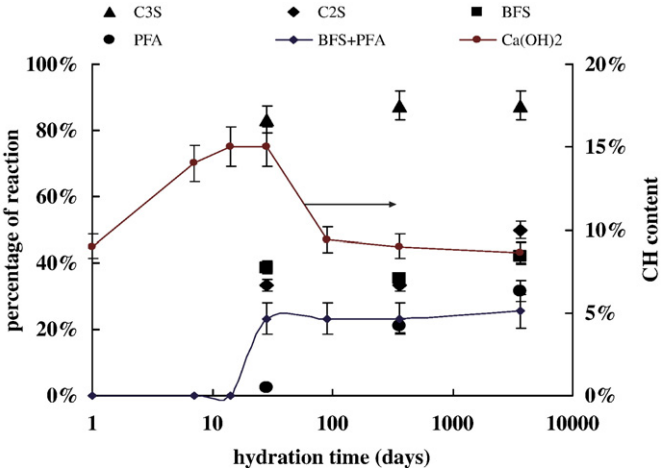

Fig. 8. Evolution versus time of the hydration of CEM V pastes ($w/c = 0.3$)

— Percentage deduced from the fits of the ^{29}Si NMR spectra and from the dissolution method.

— Portlandite content estimated from TGA.

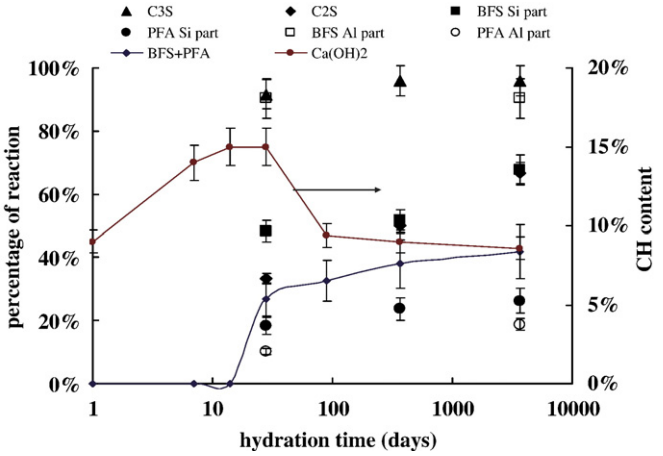

Fig. 9. Evolution versus time of the hydration of CEM V pastes ($w/c = 0.4$)

- Percentage deduced from the fits of the ^{29}Si and ^{27}Al NMR spectra and from the dissolution method.
- Portlandite content estimated from TGA.

The portlandite content increases continuously during the first 14 days of hydration corresponding to the hydration of the silicate phases of the clinker, mainly alite, when the additions (BFS and PFA) do not dissolve yet. Then between 14 and 28 days occurs the most important dissolution of the slag and the portlandite content remains constant. That means that the excess of calcium hydroxide provided by the hydration of C_3S and C_2S is exactly consumed to form C–S–H with the slag. Between 28 days and 90 days when C_3S, C_2S and the slag remain roughly constant, the portlandite content decreases due to its consumption by the fly ash which partially reacts. After 90 days, the evolution of the hydration of the CEMV pastes is very weak and slow despite the fact that the pastes are stored in saturated conditions. This demonstrates the low diffusion through the formed microstructure. The percentage of reaction of BFS and PFA deduced by the selective dissolution method reflects well the evolution deduced from the decomposition of the NMR spectra. Obviously, in this case, it is not possible to distinguish between slag and PFA and more between their silicate and aluminate parts. Nevertheless the general trend is well captured.

4. Conclusion

^{29}Si and ^{27}Al MAS NMR spectroscopies have been shown to be valuable tools for the identification of anhydrous and hydrated phases in recent and old hydrated CEM V pastes. The four silicate materials (alite, belite, PFA and BFS) present in the anhydrous cement have been characterized by ^{29}Si MAS NMR for getting reference spectra. From the simulation of ^{29}Si NMR spectra of CEM V cement, quantitative information were obtained for silicate phases present in the CEM V before and after long time hydration (10 years).

The clinker components especially alite have quickly reacted contrary to slag and especially fly ash of whom the hydration is delayed. In particular the hydration of PFA is the weakest in the cement and BFS represents the major part of hydration of SCMs in the material. The difference between the hydration for each component is important and can vary from a very weak hydration degree (only few percent for PFA) to a quasi complete hydration for C_3S. The percentage of hydrated phases is about 50% after 28 days and remains quasi constant after 10 years meaning a rather incomplete hydration reaction in CEM V cement.

^{27}Al MAS NMR allowed to characterize the main aluminate phases (C_3A, C_4AF, PFA and BFS) by their quadrupolar parameters and their different isotropic chemical shifts that have been used to distinguish between anhydrous and hydrated phases in the material. In anhydrous CEM V cement it appears from our simulations that aluminium is essentially present as tetrahedral sites in PFA and BFS. The spectra of hydrated samples ($w/c = 0.4$) after 1 month are quite different from the anhydrous but without further noticeable modifications after 10 years. Our results showed that the aluminate part of BFS has practically fully reacted at 28 days when the PFA content only slightly decreased. Al is present in hydrated materials in AFt and AFm phases and also in Al (IV) sites incorporated in C–S–H which represent about 40% of Al in the hydrated materials. While less quantitative, the chemical methods such thermal analysis for the determination of calcium hydroxide content and selective dissolution method to estimate the degree of reaction of SCMs, allow to catch easily the major trends of the evolution. Finally, even cured in wet conditions, old CEM V paste is far from being fully hydrated proving the peculiar microstructure of this kind of material.

References

[1] J. Bensted, P. Barnes, Structure and Performance of Cements, Spon Press, London, 2002.
[2] H.F.W. Taylor, Cement Chemistry, 2nd ed. Telford Publishing, London, 1997.
[3] D.X. Li, S. Jinlin, C. Yimin, C. Lin, W. Xuequan, Study of properties on fly ash–slag complex cement, Cem. Concr. Res. 30 (2001) 1381–1387.
[4] P. Lovera, C. Galle, P. Le Bescop, Conference MRS 2000, Sydney, Australia, 2000.
[5] P. Colombet, A.R. Grimmer, H. Zanni, P. Sozanni, Nuclear Magnetic Resonance Spectroscopy of Cement-Based Materials, Springer, Berlin, 1998.
[6] G. Engelhardt, D. Michel, High-Resolution Solid-State NMR of Silicates and Zeolites, Wiley, Chichester, 1987 chapter 4.
[7] E. Lippmaa, M. Mägi, A. Samoson, G. Engelhardt, A.R. Grimmer, Structural studies of silicates by solid-state high-resolution ^{29}Si NMR J, Am. Chem. Soc. 102 (1980) 4889–4893.
[8] R.J. Kirkpatrick, X.D. Cong, An introduction to ^{27}Al and ^{29}Si NMR spectroscopy of cements and concretes, Application of NMR Spectroscopy to Cement Science, Gordon and Breach, Amsterdam, 1993, pp. 55–75.
[9] J. Skibsted, J. Jakobsen, Characterization of the calcium silicate and aluminate phases in anhydrous and hydrated Portland cements by ^{27}Al and ^{29}Si MAS NMR spectroscopy, NMR Spectroscopy of Cement-Based Materials, Springer, 1998, pp. 3–45.
[10] J. Skibsted, C. Hall, Characterization of cement minerals, cements and their reaction products at the atomic and nano scale, Cem. Concr. Res 38 (2008) 205–225.
[11] J. Skibsted, H.J. Jakobsen, C. Hall, Quantification of calcium phases in Portland cements by ^{29}Si MAS NMR spectroscopy, J. Chem. Soc. Faraday trans. 91 (1995) 4423–4430.
[12] J. Skibsted, O.M. Jensen, H.J. Jakobsen, Hydration kinetics for the alite, belite, and calcium aluminate phase in Portland cements from ^{27}Al and ^{29}Si MAS NMR spectroscopy, Proc. 10th Int. Congr. Chem. Cem. Gothenburg, Sweden, vol. 2, 1997, paper 2ii056.
[13] J. Hjorth, J. Skibsted, J. Jakobsen, ^{29}Si MAS NMR studies of Portland cement components and effects of microsilica on the hydration reaction, Cem. Concr. Res. 18 (1988) 789–798.
[14] J. Skibsted, E. Henderson, H.J. Jakobsen, Characterization of calcium aluminate phases in cements by ^{27}Al MAS NMR spectroscopy, Inorg. Chem. 32 (1993) 1013–1027.
[15] J. Skibsted, H.J. Jakobsen, C. Hall, Direct observation of aluminium guest ions in the silicate phases of cement minerals by ^{27}Al MAS NMR spectroscopy, J. Chem. Soc. Faraday Trans. 90 (14) (1994) 2095–2098.
[16] M.D. Andersen, H.J. Jakobsen, J. Skibsted, Characterization of white Portland cement hydration and the C–S–H structure in the presence of sodium aluminate by ^{27}Al and ^{29}Si MAS NMR spectroscopy, Cem. Concr. Res. 43 (2004) 857–868.
[17] P. Faucon, T. Charpentier, D. Bertrandie, A. Nonat, J. Virlet, J.C. Petit, Characterization of calcium aluminate hydrates of cement pastes by ^{27}Al MQ-MAS NMR, Inorg. Chem. 37 (15) (1998) 3726–3733.
[18] P. Faucon, T. Charpentier, A. Nonat, J.C. Petit, Triple-quantum two-dimensional 27Al magic angle nuclear magnetic resonance study of the aluminium incorporation in calcium silicate hydrates, J. Am. Chem. Soc. 120 (1998) 12075–12082.
[19] M.D. Andresen, H.J. Jakobsen, J. Skibsted, Incorporation of aluminium in the calcium silicate hydrate (C–S–H) of hydrated Portland cements: a high-field ^{27}Al and ^{29}Si MAS NMR investigation, Inorg. Chem. 42 (2003) 2280–2287.
[20] M.D. Andersen, H.J. Jakobsen, J. Skibsted, A new aluminium hydrate species in hydrated Portland cements characterized by ^{29}Si and ^{27}Al MAS NMR spectroscopy, Cem. Concr. Res. 36 (2005) 3–17.
[21] D. Müller, W. Gessner, H.J. Behrens, G. Scheler, Determination of the aluminium coordination in aluminium–oxygen compounds by solid-state high-resolution ^{27}Al NMR, Chem. Phys. Lett. 79 (1981) 59–62.
[22] G.K. Sun, J.F. Young, R.J. Kirkpatrick, The role of Al in C–S–H: NMR, and XRD compositional results for precipitated samples, Cem. Concr. Res. 36 (2006) 18–29.
[23] H.M. Dyson, I.G. Richardson, A.R. Brough, A combined ^{29}Si MAS NMR selective dissolution technique for the quantitative evaluation of hydrated blast furnace slag cement blends, J. Am. Ceram. Soc. 90 (2) (2007) 598–602.
[24] T. Charpentier, PhD, Thesis University Paris XI, France (1998).

[25] a) F. Angeli, M. Gaillard, P. Jolivet, T. Charpentier, Contribution of ^{43}Ca MAS NMR for probing the structural configuration of calcium in glass, Chem. Phys. Lett. 440 (4–6) (2007) 324–328;
b) B. Bureau, G. Silly, J.Y. Buzaré, C. Legein, D. Massiot, From crystalline to glassy gallium fluoride materials: an NMR study of ^{69}Ga and ^{71}Ga quadrupolar nuclei, Solid State Nucl. Magn. Reson. 14 (1999) 181.
[26] K. Luke, F.P. Glasser, Internal chemical evolution of the constitution of blended cements, Cem. Concr. Res. 18 (4) (1988) 495–502.
[27] K.H. Jost, B. Ziemer, R. Seydel, Redetermination of the structure of β-dicalcium silicate, Acta Crystallogr., B 33 (1977) 1696–1700.
[28] N.I. Golovastikov, R.G. Matveeva, N.V. Belov, Sov. Phys. Crystallogr. 20 (4) (1975) 441–445.
[29] J. Schneider, M.A. Cincotto, H. Panepucci, ^{29}Si and ^{27}Al high-resolution NMR characterization of calcium silicate hydrate phases in activated blast-furnace slag pastes, Cem. Concr. Res. 31 (2001) 993–1001.
[30] S.D. Wang, K.L. Scrivener, ^{29}Si and ^{27}Al NMR study of alkali-activated slag, Cem. Concr. Res. 33 (2003) 769–774.
[31] S. Murgier, H. Zanni, D. Gouvenot, Blast furnace slag cement: a ^{29}Si and ^{27}Al NMR study, C.R. Chimie 7 (2004) 389–394.
[32] S.L. Poulsen, V. Kocaba, G. Le Saoût, H.J. Jakobsen, K.L. Scrivener, J. Skibsted, Improved quantification of alite and belite in anhydrous Portland cements by ^{29}Si MAS NMR: effects of paramagnetic ions, Solid State Nucl. Magn. Reson. 36 (2009) 32–44.
[33] A. Kubo, T.P. Spaniol, T. Terao, The effect of bulk magnetic susceptibility on solid state NMR spectra of paramagnetic compounds, J. Magn. Reson. 133 (2) (1998) 330–340.
[34] J. Skibsted, H. Bildsoe, H.J. Jakobsen, High-speed spinning versus high magnetic field in MAS NMR of quadrupolar nuclei ^{27}Al MAS NMR of $3CaO.Al_2O_3$, J. Magn. Reson. 92 (1991) 669–676.
[35] D. Massiot, B. Cote, F. Taulelle, J.P. Coutures, Application of NMR Spectroscopy to Cement Science, Gordon and Breach, Amsterdam, 1994, pp. 153–169.
[36] E. Oldfied, R.A. Kinsey, K.A. Smith, J.A. Nichols, R.J. Kirkpatrick, High-resolution NMR of inorganic solids. Influence of magnetic centers on magic-angle sample-spinning lineshapes in some natural aluminosilicates, J. Magn. Reson. 51 (1983) 325–329.
[37] H.J. Jakobsen, H. Jacobsen, H. Lindgreen, Solid-State ^{27}Al and ^{29}Si MAS NMR studies on diagenesis of mixed layer silicates in oil source rocks, Fuel 67 (1988) 727–730.
[38] J. Skibsted, H.J. Jakobsen, C. Hall, Quantitative aspects of ^{27}Al MAS NMR of calcium aluminoferrites, Adv. Cem. Based Mater. 7 (1998) 57–59.
[39] A.A. Colville, S. Geller, Crystal structure of brownmillerite, Ca_2FeAlO_5, Acta Crystallogr., Cryst. B 27 (1971) 2311–2315.
[40] D. Müller, A. Rettel, W. Gessner, G.J. Scheler, An application of solid-state magic-angle spinning ^{27}Al NMR to the study of cement hydration, J. Magn. Reson. 57 (1984) 152–156.
[41] D. Müller, W. Gessner, A. Samoson, E. Lippmaa, Solid-state ^{27}Al NMR studies on polycrystalline aluminates of the system $CaO–Al_2O_3$, Polyhedron 5 (3) (1986) 779–785.
[42] A. Brough, C.J. Dobson, Applications of selective ^{29}Si isotopic enrichment to studies of the structure of calcium silicate hydrate (C–S–H) gels, J. Am. Ceram. Soc. 77 (1994) 593–596.
[43] X. Cong, R.J. Kirkpatrick, J.L. Yarger, P.F. McMillan, The structure of calcium silicate hydrate: NMR and Raman spectroscopic results, NMR Spectroscopy of Cement-Based Materials, Springer, 1998, pp. 143–158.
[44] S. Masse, H. Zanni, J. Lecourtier, J.C. Roussel, A. Rivereau, ^{29}Si solid state NMR study of tricalcium silicate and cement hydration at high temperature, Application of NMR Spectroscopy to Cement Science, Gordon and Breach, Amsterdam, 1993, pp. 249–257.
[45] I. Klur, B. Pollet, J. Virlet, A. Nonat, C–S–H structure evolution with calcium content by multinuclear NMR, NMR Spectroscopy of Cement-Based Materials, Springer, 1998, pp. 119–142.
[46] F. Brunet, Ph. Bertani, T. Charpentier, A. Nonat, J. Virlet, Applications of 29Si homonuclear and 1H–29Si heteronuclear NMR correlation to structural studies of calcium silicate hydrates, J. Phys. Chem. B 108 (2004) 15494–15502.
[47] M. Mägi, E. Lippmaa, A. Samoson, G. Engelhardt, A. Grimmer, Solid-state high-resolution silicon ^{29}Si chemical shifts in silicates, J. Phys. Chem. 88 (1984) 1518–1522.
[48] I.G. Richardson, A.R. Brough, R. Brydson, G.W. Groves, C.M. Dobson, Location of aluminium in substituted calcium silicate hydrate (C–S–H) gels as determined by ^{29}Si and ^{27}Al NMR and EELS, J. Am. Ceram. Soc. 76 (1993) 2285–2288.
[49] H. Stade, D. Müller, On the coordination of Al in ill-crystallized C–S–H phases formed by hydration of tricalcium silicate and by precipitation reactions at ambient temperature, Cem. Concr. Res. 17 (1987) 553–561.